Semiconductor Physics, Quantum Electronics & Optoelectronics, 2010. V. 13, N 4. P. 41-50.

PACS 78.20.Fm, 87.64.-t

Degree of local depolarization determined for fields of laser radiation scattered by multilayer birefringentnetworks of protein crystals

Yu.A. Ushenko[1], A.P. Angelsky[2]
[1]*Chernivtsi National University, Department for Correlation Optics, 2, vul. Kotsyubins'kogo, 58012 Chernivtsi, Ukraine; yuriyu@gmail.com*
[2]*Chernivtsi National University, Department for Optics and Spectroscopy, 2, vul. Kotsyubins'kogo, 58012 Chernivtsi, Ukraine*

Abstract. Represented in this work are theoretical basics for description of fields created by scattered coherent radiation with using the new correlation parameter – degree of local depolarization (DLD). The authors have adduced data of measurements of coordinate distributions for DLD in laser images of healthy and pathologically changed skin of a rat. Investigated are the values and ranges of changes in statistical (moments of the first to fourth orders), correlation (correlation area) and fractal (slopes and dispersion of extremes of logarithmic dependences for power spectra) parameters of coordinate distributions for DLD. Defined are objective criteria for diagnostics of oncological changes in the structure of rat skin.

Keywords: laser, polarization, complex degree of coherency, birefringence, correlation, statistical moments, fractal.

Manuscript received 10.09.10; accepted for publication 02.12.10; published online 28.02.11.

1. Introduction

By tradition, light scattering processes in phase-inhomogeneous biological objects are considered in a statistical approach (theory of radiation transfer [1], Monte-Carlo modeling [2]).

Use of modern laser technique in investigations of biological tissues (BT) stimulates development of new approaches to an analysis and description of fields inherent to coherent radiation scattered by them. In recent 10 to 15 years, in optics of scattering media there arose a separate direction – laser polarimetry [3 – 31]. Being based on it and using the approach of single light scattering, there determined are interrelations between the set of statistical moments of the first to fourth orders [5 - 7, 11, 15, 20, 26, 27, 31], correlation functions [13, 18, 19, 22, 27], fractal dimensionalities [6, 7, 26], networks of polarization singularities [23, 29] that characterize the distribution of polarization states for laser fields, and parameters of optical anisotropy inherent to optically thin BT layers.

When multiple scattering takes place, polarization information upon the BT structure becomes ambiguous and, as a consequence, loses its diagnostic sense [9, 10, 12, 16, 19]. This phenomenon got the name of depolarization of optical radiation due to statistical averaging the polarization states [12, 16, 19]. On the other hand, when scattered is coherent laser radiation, the speckle field with 100 % degree of local polarization is formed [8]. Thereof, it seems topical to develop new correlation approaches [3, 4] to descriptions of mechanisms providing depolarization of laser radiation multiply scattered in layers of optically thick BT.

Our work is aimed at studying the possibilities for diagnostics of optically anisotropic BT components (epithelial and dermal skin layers) with application of statistical, correlation and fractal analyses for coordinate distributions inherent to local depolarization degree in the case of multiply scattered laser radiation.

2. Optical modeling for processes providing conversion of laser radiation parameters by a skin layer

As a base to analyze the structure of laser radiation field converted by a skin layer, we use the following model [5-7, 14-17, 19, 30]:

- we consider this layer as a two-component system consisting of an optically anisotropic derma and rough surface optically isotropic epithelium (Fig. 1);

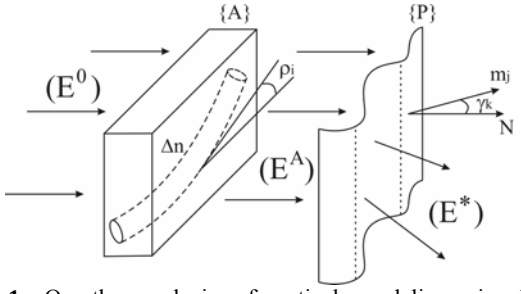

Fig. 1. On the analysis of optical modeling aimed at polarization-phase properties of the skin layer. ρ_i is the direction of fibril optical axis with the birefringence index Δn; γ_k - slope angle of the epithelium plate, which is formed by directions of micro- normal m_j and macro-normal N; (E^0), (E^A) and (E^*) - Maxwell's vectors of the illuminating laser beam scattered by the collagen network and epithelium layer.

- optical properties of the network inherent to birefringent collagen fibrils in the derma layer are characterized with the Jones matrix [27]

$$\{A\} = \begin{Vmatrix} a_{11} & a_{12} \\ a_{21} & a_{22} \end{Vmatrix}, \qquad (1)$$

where

$$a_{ik}(r,\rho,\delta) = \begin{cases} a_{11} = \cos^2\rho(r) + \sin^2\rho(r)\exp(-i\delta(r)); \\ a_{12} = a_{21} = \cos\rho(r)\sin\rho(r)(1-\exp(-i\delta(r))); \\ a_{22} = \sin^2\rho(r) + \cos^2\rho(r)\exp(-i\delta(r)). \end{cases} \qquad (2)$$

Here, ρ is the direction of optical axis; $\delta = 2\pi/\lambda\,\Delta n d$ - phase shift between amplitude orthogonal components; λ - wavelength; d - geometric distance; Δn - index of birefringence.

- optical properties of surface epithelium plane plates are characterized with the Jones operator of the following look [16, 19]

$$\{P\} = \begin{vmatrix} p_x/p_y & 0 \\ 0 & 1 \end{vmatrix}; \qquad (3)$$

- net Jones matrix for the skin layer $\{D\}$ is determined with the product of partial operators (1) and (3)

$$\{D\} = \{P\}\{A\} = \begin{Vmatrix} p_{11} & p_{12} \\ p_{21} & p_{22} \end{Vmatrix} \times \begin{Vmatrix} a_{11} & a_{12} \\ a_{21} & a_{22} \end{Vmatrix} = \\ = \begin{Vmatrix} (p_{11}a_{11} + p_{12}a_{21}) & (p_{11}a_{12} + p_{12}a_{22}) \\ (p_{21}a_{11} + p_{22}a_{21}) & (p_{21}a_{12} + p_{22}a_{22}) \end{Vmatrix}. \qquad (4)$$

- conversion processes for the amplitude (E_x, E_y) and phase δ of laser radiation in the skin layer are described with the following matrix equation

$$(E) = \{D\}\left(E^{(0)}\right) \leftrightarrow \begin{pmatrix} E_x \\ E_y \end{pmatrix} = \begin{Vmatrix} d_{11} & d_{12} \\ d_{21} & d_{22} \end{Vmatrix} \begin{pmatrix} E_x^{(0)} \\ E_y^{(0)} \end{pmatrix}, \qquad (5)$$

where $\left(E^{(0)}\right)$ and (E) are the Jones vectors for illuminating and converted laser beams;

$$\begin{pmatrix} E_x^{(0)} \\ E_y^{(0)} \end{pmatrix} = \begin{pmatrix} U_x^{(0)} \\ U_y^{(0)}\exp\left(-i\delta_{xy}^{(0)}\right) \end{pmatrix}; \quad \begin{pmatrix} E_x \\ E_y \end{pmatrix} = \begin{pmatrix} U_x \\ U_y\exp\left(-i\delta_{xy}\right) \end{pmatrix}; \qquad (6)$$
$$\delta_{xy}^{(0)} = \delta_x^{(0)} - \delta_y^{(0)}; \;\; \delta_{xy} = \delta_x - \delta_y .$$

Here, δ_{xy} is the phase shift between real parts U_x, U_y of orthogonal components E_x, E_y of laser wave;

- polarization-phase properties of every field point in the case of laser radiation scattered in skin are described with the coherence matrix $\{J\}$ [18, 19, 25]

$$\{J\} = \begin{Vmatrix} J_{xx} & J_{xy} \\ J_{yx} & J_{yy} \end{Vmatrix} = \begin{Vmatrix} E_x E_x^* & E_x E_x^* \\ E_x E_x^* & E_y E_y^* \end{Vmatrix} = \\ = \begin{Vmatrix} (U_x)^2 & U_x U_y \exp(-i\delta_{xy}) \\ U_x U_y \exp(i\delta_{xy}) & (U_y)^2 \end{Vmatrix}. \qquad (7)$$

Using the operator $\{J(r)\}$, let us characterize the polarization degree $T(r)$ of the scattered radiation field with the classic expression {4, 18]

$$T(r) = \sqrt{1 - \frac{4\left[\left\langle E_x(r,\tau)E_x^*(r,\tau)\right\rangle\left\langle E_y(r,\tau)E_y^*(r,\tau)\right\rangle - \left\langle E_x(r,\tau)E_y^*(r,\tau)\right\rangle\left\langle E_y(r,\tau)E_x^*(r,\tau)\right\rangle\right]}{\left[\left\langle E_x(r,\tau)E_x^*(r,\tau)\right\rangle + \left\langle E_y(r,\tau)E_y^*(r,\tau)\right\rangle\right]^2}}. \qquad (8)$$

Here $\langle\ \rangle$ denotes the operation of averaging by time.

In our case of the field inherent to scattered coherent radiation ($\langle E\rangle = E$) and ($\langle\delta_{xy}\rangle = \delta_{xy}$), the expression (8) is transformed to some constant

$$T(r) = \sqrt{1 - \frac{4\left[E_x(r)E_x^*(r)E_y(r)E_y^*(r) - E_x(r)E_y^*(r)E_y(r)E_x^*(r)\right]}{\left[E_x(r)E_x^*(r) + E_y(r)E_y^*(r)\right]^2}} = 1.0. \qquad (9)$$

In other words, all the points of polarization-inhomogeneous field of scattered laser radiation are 100 % polarized, $T(r) = 1.0$.

3. Correlation nature of the depolarization degree for the field of laser radiation

In [4], to describe depolarization of these fields, the authors offered another, "two-point" correlation approach. The main its idea consists in determining the degree of correlation similarity between orthogonal components E_x, E_y of laser wave amplitudes in the points r_1 and r_2 within the field of scattered coherent radiation [22, 27]. To qualitatively estimate this

similarity, they used the parameter of a complex degree of coherency (CDC)

$$\mu(r_1,r_2)=\left[\frac{Tr\left(W^{\Diamond}(r_1,r_2)W(r_1,r_2)\right)}{TrW(r_1,r_1)\cdot TrW(r_2,r_2)}\right]. \qquad (10)$$

Here, $W(r_1,r_2)$ is the transversally spectral density matrix

$$W(r_1,r_2)=\begin{bmatrix} E_x^*(r_1)E_x(r_2) & E_x^*(r_1)E_y(r_2) \\ E_y^*(r_1)E_x(r_2) & E_y^*(r_1)E_y(r_2)\end{bmatrix}, \qquad (11)$$

where $W^{\Diamond}(r_1,r_2)$ is the Hermitian conjugated matrix to the matrix $W(r_1,r_2)$; Tr - matrix spur.

Let us consider the possibility to use the above correlation approach in description of a polarization-inhomogeneous field formed by the layer of optically anisotropic derma (relations (1), (2)) with a rough surface (relation (3)). With this purpose, let us rewrite the expression (11) in the following manner

$$W_{out}(r)=D^{\Diamond}(r)\cdot W_{in}(r)\cdot D(r). \qquad (12)$$

Here, $D(r)$ is the Jones matrix (4) for the skin layer in the point r; $D^{\Diamond}(r)$ - Hermitian conjugated Jones' matrix; $W_{in}(r)$ transversally spectral density matrix for the probing beam

$$W_{in}(r)=\begin{bmatrix} E_x^{(0)*}(r)E_x^{(0)}(r) & E_x^{(0)*}(r)E_y^{(0)}(r) \\ E_y^{(0)*}(r)E_x^{(0)}(r) & E_y^{(0)*}(r)E_y^{(0)}(r)\end{bmatrix}. \qquad (13)$$

Our analysis of the complex expression (12) with account of (1) – (4) and (12), (13) enabled us to reveal that the CDC module $|\mu(r)|$ in every point r of the scattered coherent radiation field is a constant value coinciding with the polarization degree $T(r)$

$$|\mu(r)|=T(r)=1.0. \qquad (14)$$

On the other hand, some new additional information possibility to describe scattered laser radiation is brought by the phase $\Phi(\mu(r))\equiv\Phi(r)$ of CDC that is determined as

$$\Phi(r)=\frac{2U_x(r)U_y(r)\cos\delta_{xy}(r)}{U_x^2(r)+U_y^2(r)}. \qquad (15)$$

An explicit form of the value $\delta_{xy}(r)$ for the phase shift between amplitude orthogonal components $U_x(r),U_y(r)$ for laser wave in the point r can be determined from the matrix equation (5):

$$\delta_{xy}(r)=arctg\left\{\frac{\mathrm{Im}\left[d_{11}(r)E_x^{(0)}+d_{12}(r)E_y^{(0)}\right]}{\mathrm{Re}\left[d_{11}(r)E_x^{(0)}+d_{12}(r)E_y^{(0)}\right]}\right\}- arctg\left\{\frac{\mathrm{Im}\left[d_{21}(r)E_x^{(0)}+d_{22}(r)E_y^{(0)}\right]}{\mathrm{Re}\left[d_{21}(r)E_x^{(0)}+d_{22}(r)E_y^{(0)}\right]}\right\}. \qquad (16)$$

Let us rewrite the expression (16) (without reduction in analysis completeness) for the case when the skin layer is illuminated with a laser wave linearly polarized with the azimuth 0^0 ($E_x^{(0)}\equiv 1.0; E_y^{(0)}=0$)

$$\begin{aligned}\delta_{xy}(r)&=arctg\left\{\frac{\mathrm{Im}(p_{11}a_{11})}{\mathrm{Re}(p_{11}a_{11})}\right\}-arctg\left\{\frac{\mathrm{Im}(a_{21})}{\mathrm{Re}(a_{21})}\right\}= \\ &arctg\left\{\frac{\mathrm{Im}\left(\cos^2\rho-\sin^2\rho\exp(-i\delta_x)\right)}{\mathrm{Re}\left(\cos^2\rho-\sin^2\rho\exp(-i\delta_x)\right)}\right\}- \\ &-arctg\left\{\frac{\mathrm{Im}\left(\cos\rho\sin\rho\left(1-\exp(-i\delta_y)\right)\right)}{\mathrm{Re}\left(\cos\rho\sin\rho\left(1-\exp(-i\delta_y)\right)\right)}\right\}= \\ &arctg\left\{\frac{\sin^2\rho\sin\delta_x}{1-\sin^2\rho(1-\cos\delta_x)}\right\}-arctg\left\{\frac{\sin\delta_y}{1+\cos\delta_y}\right\}.\end{aligned} \qquad (17)$$

As seen from the analysis of (17), the dominant role in formation of phase modulation inherent to the field of scattered laser radiation is played by the subsurface birefringent layer of collagen fibrils. Moreover, the range of changes in phase shifts $\delta_{xy}(r)$ is maximum high

$$0\le\delta_{xy}\le\pi. \qquad (18)$$

The condition (18) corresponds to the following range of changes in CDC phase:

$$0\le\Phi(r)\le 1.0. \qquad (19)$$

Thus, to use the parameter $\Phi(r)$ is efficient when determining the measure of correlation between orthogonal components of the complex amplitude in different points r within the field of scattered laser radiation. In this sense, this parameter $\Phi(r)$ will be named as the degree of local depolarization (DLD) for points of polarization-inhomogeneous coherent field.

4. Optical setup and method for measuring thr degree of local depolarization in the field of scattered laser radiation

Shown in Fig. 2 is the optical setup for measuring coordinate distributions of DLD in the field of laser light transformed by a skin layer [5]. As objects for investigation, we used optically thick (geometric thickness $d=75$ μm, extinction coefficient $\tau\le 0.75$) histological sections of rat skin prepared using the standard technique with a freezing microtome [4].

Illumination of the rat skin histological sections was made by a parallel beam (Ø $=10^4$ μm) of the He-Ne laser (λ = 0.6328 μm) 1. Using the polarizer 4 and quarter-wave plate 5, we could form arbitrary states of polarization for the probing laser beam. The image of the skin samples 6 was projected with the micro-objective 7 onto the plane of light-sensitive area ($r\equiv m\times n=800\,pix\times 600\,pix$) of CCD camera 10.

The method of measuring coordinate distributions of DLD $\Phi(r)$ consists of the following stages:

1. The transmission plane of the polarizer-analyzer 9 is sequentially oriented under the angles $\Theta = 0^0$, $\Theta = 90^0$ and measured are the respective discrete $(m \times n)$ sets of values for intensities $I_0\begin{pmatrix} r_{11} & \dots & r_{1m} \\ \dots & \dots & \dots \\ r_{n1} & \dots & r_{nm} \end{pmatrix}$, $I_{90}\begin{pmatrix} r_{11} & \dots & r_{1m} \\ \dots & \dots & \dots \\ r_{n1} & \dots & r_{nm} \end{pmatrix}$.

2. Using rotation of the analyzer transmission plane within the limits $\Theta = 0^0 \div 180^0$, one determines a set of values for maximum and minimum intensity levels $I_{\max}\begin{pmatrix} r_{11} & \dots & r_{1m} \\ \dots & \dots & \dots \\ r_{n1} & \dots & r_{nm} \end{pmatrix}$, $I_{\min}\begin{pmatrix} r_{11} & \dots & r_{1m} \\ \dots & \dots & \dots \\ r_{n1} & \dots & r_{nm} \end{pmatrix}$ for every separate pixel of the CCD camera as well as respective rotation angles $\Theta\begin{pmatrix} r_{11} & \dots & r_{1m} \\ \dots & \dots & \dots \\ r_{n1} & \dots & r_{nm} \end{pmatrix}\left(I\begin{pmatrix} r_{11} & \dots & r_{1m} \\ \dots & \dots & \dots \\ r_{n1} & \dots & r_{nm} \end{pmatrix} \equiv I_{\min} \right)$.

3. Then, calculated are the coordinate distributions for the azimuth and ellipticity of laser field polarization

$$\alpha\begin{pmatrix} r_{11} & \dots & r_{1m} \\ \dots & \dots & \dots \\ r_{n1} & \dots & r_{nm} \end{pmatrix} = \Theta\left(I_{\min}(r)\right) - \frac{\pi}{2}; \qquad \beta\begin{pmatrix} r_{11} & \dots & r_{1m} \\ \dots & \dots & \dots \\ r_{n1} & \dots & r_{nm} \end{pmatrix} = arctg\frac{I(r)_{\min}}{I(r)_{\max}}. \tag{20}$$

4. Using (20), one calculates the coordinate distributions for phase shifts $\delta\begin{pmatrix} r_{11} & \dots & r_{1m} \\ \dots & \dots & \dots \\ r_{n1} & \dots & r_{nm} \end{pmatrix}$

$$\delta(r) = arctg\left[\frac{tg2\beta(r)}{tg\alpha(r)}\right]. \tag{21}$$

5. The coordinate distribution of DLD $\Phi\begin{pmatrix} r_{11} & \dots & r_{1m} \\ \dots & \dots & \dots \\ r_{n1} & \dots & r_{nm} \end{pmatrix}$ can be obtained using the following relation

$$\Phi(r) = arctg\frac{I_0^{0,5}(r)I_{90}^{0,5}(r)\cos\delta(r)}{I_0(r) + I_{90}(r)}. \tag{22}$$

5. Algorithms for statistical, correlation and fractal analyses of coordinate distributions for the degree of local polarization

To get an objective estimation of the coordinate distributions $\Phi(x = 1 \div m - 1; y = 1 \div n)$ inherent to laser images of histological skin sections, we used the complex statistical, correlation and fractal analysis.

The set of statistical moments of the first to fourth orders $Z^{\Phi}_{j=1,2,3,4}$ for DLD distributions was calculated using the following relations [6, 7, 26, 31]

$$Z_1^{\Phi} = \frac{1}{N}\sum_{i=1}^{N}|\Phi_i|,\ Z_2^{\Phi} = \sqrt{\frac{1}{N}\sum_{i=1}^{N}\Phi_i^2},$$

$$Z_3^{\Phi} = \frac{1}{\left(Z_2^{\Phi}\right)^3}\frac{1}{N}\sum_{i=1}^{N}\Phi_i^3,\ Z_4^{\Phi} = \frac{1}{\left(Z_2^{\Phi}\right)^4}\frac{1}{N}\sum_{i=1}^{N}\Phi_i^4. \tag{23}$$

Here, $N = m \times n$ is the number of pixels in the CCD camera.

As a base for the correlation analysis of DLD distributions we took the method of autocorrelation with using the function [19, 22, 27]

$$K^{\Phi}_{i=1\div n}(\Delta m) = \lim_{m\to 0}\frac{1}{m}\int_1^m [\Phi_i(m)][\Phi_i(m - \Delta m)]dm. \tag{24}$$

Here, $(\Delta m = 1 pix)$ is the step for changing the coordinates $x = 1 \div m$ of the DLD distribution for the separate i-th line of pixels in the digital camera.

The net expression for the autocorrelation function was obtained by averaging the partial functions (24) over all the lines $i = 1 \div n$

$$K^{\Phi}(\Delta m) = \frac{\sum_{i=1}^{n} K_i^{\Phi}(\Delta m)}{n}. \tag{25}$$

To qualitatively characterize the autocorrelation dependences $K^{\Phi}(\Delta m)$, we chose the "correlation area" S^{Φ}

$$S^{\Phi} = \int_1^m K^{\Phi}(\Delta m)dm; \tag{26}$$

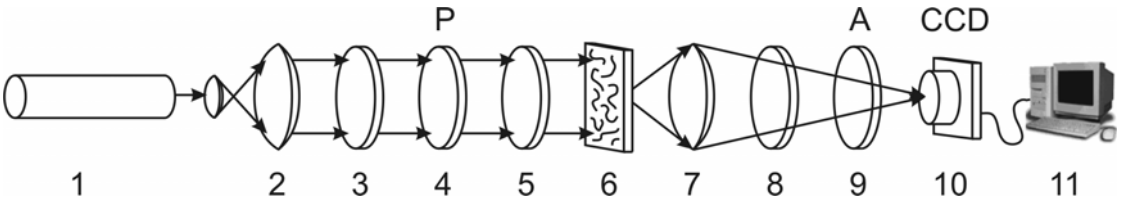

Fig. 2. Optical setup for measurements: 1 – He-Ne laser; 2 – collimator; 3, 5, 8 – quarter-wave plates; 4, 9 – polarizer and analyzer; 6 – object; 7 – micro-objective (x4); 10 – CCD camera; 11 – personal computer.

The fractal analysis of $\Phi(m\times n)$ distributions was based on calculations of the logarithmic dependences $\log J(\Phi) - \log d^{-1}$ for power spectra $J(\Phi)$

$$J(\Phi) = \int_{-\infty}^{+\infty} \Phi \cos 2\pi\nu d\nu , \qquad (27)$$

where $\nu = d^{-1}$ are the spatial frequencies that are determined by geometrical dimensions d of structural elements in the skin layer.

The dependences $\log J(\Phi) - \log d^{-1}$ were approximated using the least squares method to the curves $V(\eta)$, straight parts of which enabled us to determine the slope angles η and corresponding fractal dimensionalities F^{Φ} [6, 7]

$$F^{\Phi} = 3 - tg\eta . \qquad (28)$$

Classification of the coordinate distributions $\Phi(m\times n)$ was performed in accord with the following criteria [23]:

- $\Phi(m\times n)$ is fractal or self-similar when the slope angle is constant $\eta = const$ within the limits of 2 or 3 decades in changing the dimensions d ;
- $\Phi(m\times n)$ are multi-fractal when several slope angles of $V(\eta)$ are available;
- $\Phi(m\times n)$ is random when no stable slope angles of $V(\eta)$ are available over the whole range of changing dimensions d .

All the distributions $\log J(\Phi) - \log d^{-1}$ were characterized with the dispersion

$$D^{\Phi} = \sqrt{\frac{1}{N}\sum_{i=1}^{N}\left[\log J(\Phi) - \log d^{-1}\right]^2} . \qquad (31)$$

6. Statistical, correlation and fractal parameters of coordinate distributions for the degree of local depolarization of laser field light scattered by skin layers in different physiological states

Shown in Fig. 3 are laser images of histological sections inherent to healthy (fragment (a)) and oncologically changed (fragment (b)) rat skin obtained for crossed transmission planes ($\Theta = 90^0$) of the polarizer 4 and analyzer 9 (Fig. 2).

Our choice of the studied objects was stipulated both with fundamental and applied reasons.

From the fundamental viewpoint, the sample of skin with rough surface is a classical example of multilayer biological tissue providing simultaneous manifestation of various mechanisms (both bulk (1), (2) and surface (3)) in the scattering of coherent radiation, and one can observe polarization-inhomogeneous field.

From the applied viewpoint, the samples of rat skin allows to experimentally create oncological states and, therefore, can be efficiently used in optimization of correlation-phase laser diagnostics of pathological changes.

Our analysis of laser images corresponding to the skin of both types enabled us to reveal their phase-inhomogeneous structure (relations (6), (8) – (16)) that can be visualized with crossed polarizer and analyzer. In the case of pathologically changed skin (Fig. 3, fragment (b)), there observed is a higher level of blooming. This fact can be explained by growth of birefringence in newly created collagen fibrils [5, 8, 10, 14, 17, 24, 25, 31] as well as increasing phase modulation ($\delta_{xy}^{(\min)} \leftrightarrow \delta_{xy}^{(\max)}$) in the points of scattered radiation field. Quantitatively, these mechanisms of coherent radiation conversion are characterized by the value and range of DLD changes (relation (19)) in laser images of rat skin in different physiological states (Fig. 4).

From the obtained laser images of histological sections prepared from the skin of both types, it is seen that these are characterized with the widest ($0 \le \Phi \le 1$) range of DLD changes. At the same time, the coordinate structure of $\Phi(m\times n)$ distributions is rather complex and individual both for healthy (fragment (a)) and oncologically changed (fragment (b)) skin.

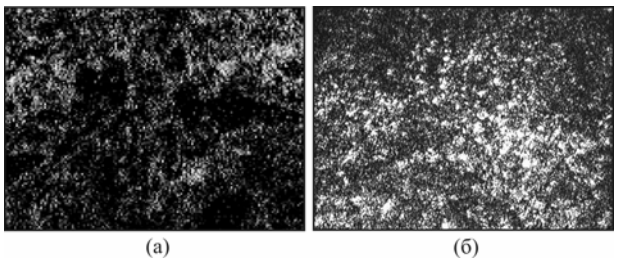

Fig. 3. Laser images of histological sections inherent to healthy (a) and oncologically changed (carcinoma) (b) rat skin.

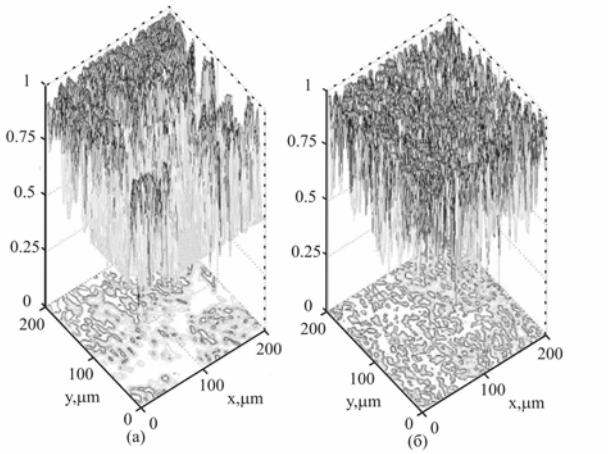

Fig. 4. Coordinate distributions $\Phi(m\times n)$ of laser images for healthy (fragment (a)) and oncologically changed (fragment (b)) skin.

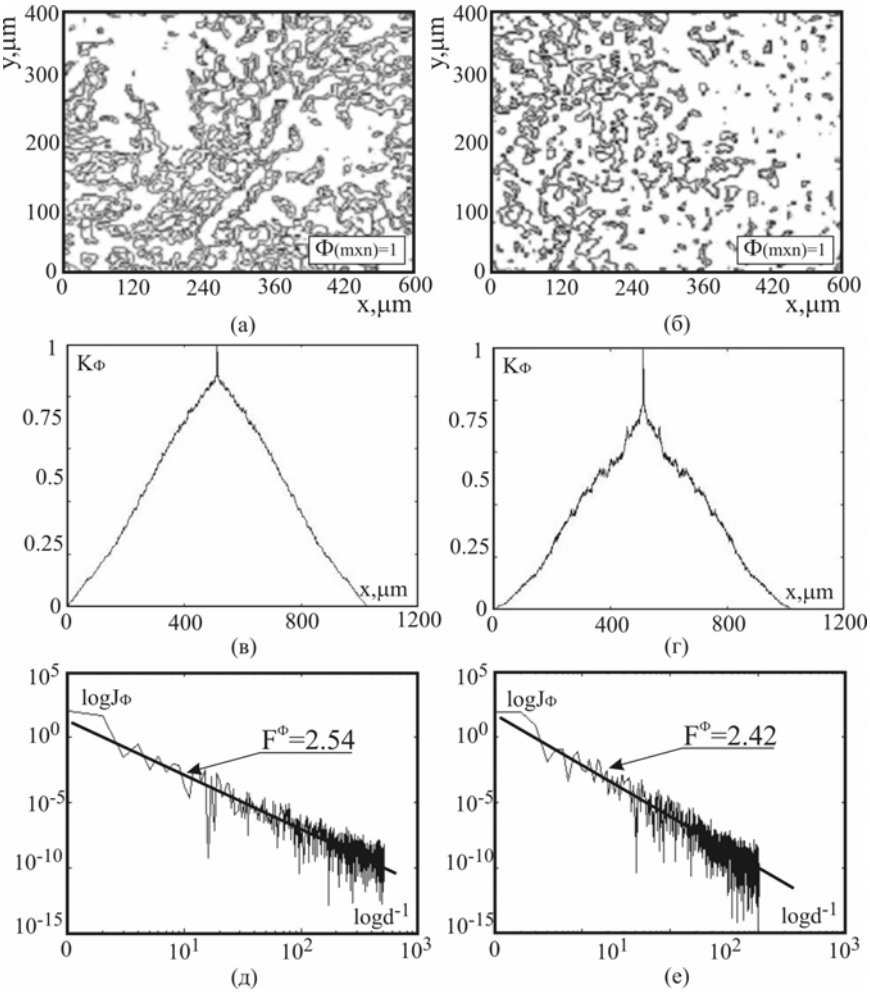

Fig. 5. Coordinate (fragments (a), (b)), correlation (fragments (c), (d)) and fractal (fragments (e), (f)) structures of the sampling Φ(*m*×*n*) = 1 of two-dimensional DLD distributions in laser images of histological sections of healthy rat (fragments (a), (c), (e)) and that sick of cancer (fragments (b), (d), (f)). See explanations in the text.

To determine statistical (relation (23)), correlation (relations (24)) and fractal (relations (26) – (28)) parameters of coordinate DLD distributions sensitive to changes in the structure of laser images, we used the following method of information selection. From the whole $\Phi(m \times n)$ set, we chose characteristic or extreme values:

- "minimal" ($\Phi_{\min} = 0$) that correspond to absence of phase modulation ($\delta_{xy} = 0$, relation (15)) of orthogonal components inherent to the laser wave amplitude. From the physical viewpoint, this sampling corresponds to mechanisms of radiation transformation (extinction) by the optically isotropic skin component;
- "mean" ($\widetilde{\Phi} = 0.5$) that correspond to the phase shifts ($\widetilde{\delta} = \pi/3$) formed by the network of collagen fibrils with the averaged statistical dimensions $d \approx 75 \mu m$, and the birefringence index $\Delta n = 1.5 \times 10^{-3}$. This sampling of DLD values is characteristic both to the healthy and pathologically changed optically anisotropic component of skin derma [14, 17, 30];
- "maximal" ($\Phi_{\max} = 1$) that correspond to extreme phase shifts ($\delta_{xy} = \pi/2$). In our opinion, this level of phase modulation is more probable for some sub-ensemble of "newly-created" skin derma fibrils in the process of carcinoma formation.

Within the limits of every column $\left(1_{pix} \times n_{pix}\right)^{(k=1,\ 2,\ \ldots,\ m)}$ of two-dimensional array $\Phi(m \times n)$ by scanning along the horizontal direction $x \equiv 1,\ \ldots,\ m$ with the step $\Delta x = 1 pix$, we calculated the amount (N) of values $\Phi_{\min}$, – ($N_{\min}^{(k)}$); $\widetilde{\Phi}$, – ($\widetilde{N}^{(k)}$) and $\Phi_{\max}$, – ($N_{\max}^{(k)}$).

Thus, we determined the dependences $N_{\min}(x) \equiv (N_{\min}{}^{(1)},\ N_{\min}{}^{(2)},\ \ldots,\ N_{\min}{}^{(m)})$; $\widetilde{N}(x) \equiv (\widetilde{N}^{(1)},\ \widetilde{N}^{(2)},\ \ldots,\ \widetilde{N}^{(m)})$ and

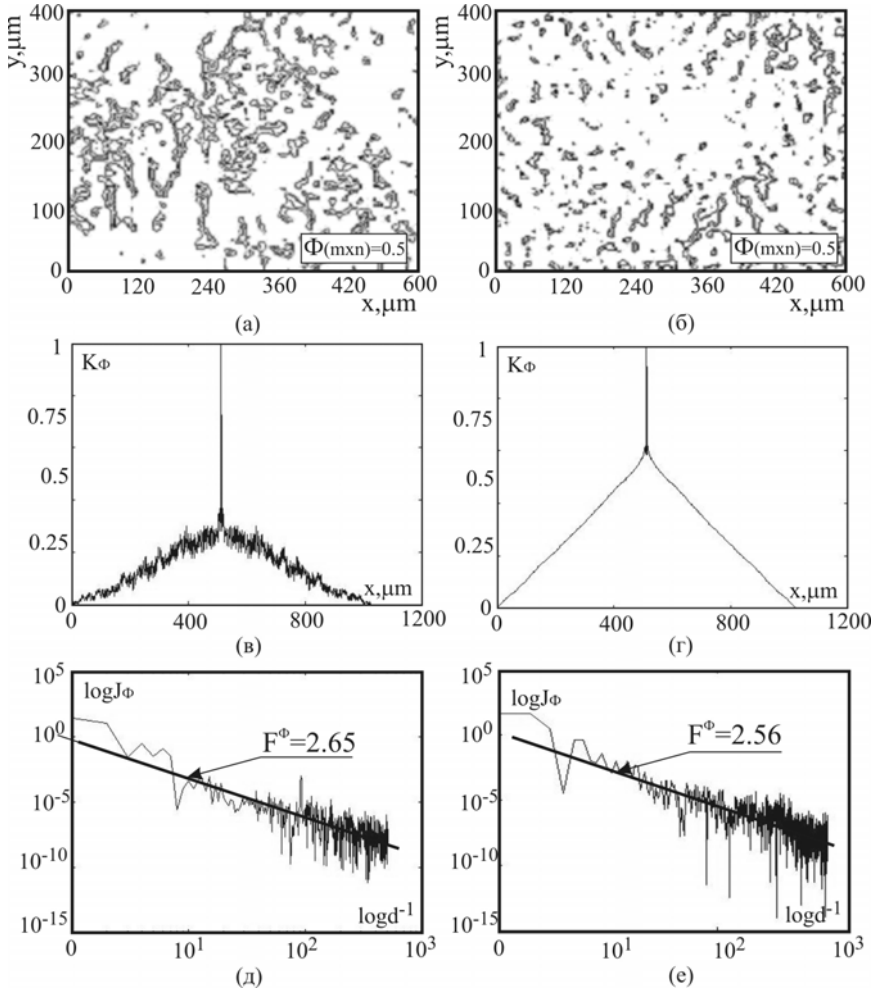

Fig. 6. Coordinate (fragments (a), (b)), correlation (fragments (c), (d)) and fractal (fragments (e), (f)) structures of the sampling $\Phi(m\times n) = 0.5$ for two-dimensional DLD distributions corresponding to laser images of histological sections taken from healthy rat (fragments (a), (c), (e)) and that sick with cancer (fragments (b), (d), (f)). See explanations in the text.

$N_{\max}(x) \equiv (N_{\max}{}^{(1)},\ N_{\max}{}^{(2)},\ ...,\ N_{\max}{}^{(m)})$ of the amount of extreme DLD values within the limits of a laser image for a skin histological section.

Shown in Fig.5 to Fig. 7 are $\Phi_{\min}(m\times n)$ samplings (Fig. 5, fragments (a), (b)); $\widetilde{\Phi}(m\times n)$ (Fig. 6, fragments (a), (b)); $\Phi_{\max}(m\times n)$ (Fig. 7, fragments (a), (b)); autocorrelation functions $K_{\min}(\Delta x)$, $\widetilde{K}(\Delta x)$, $K_{\max}(\Delta x)$ (fragments (c), (d)) as well as logarithmic dependences $\log N_{\min}, \widetilde{N}, N_{\max} - \log d^{-1}$ for power spectra of distributions $N_{\min}(x)$, $\widetilde{N}(x)$, $N_{\max}(x)$ (fragments (e), (f)), which characterize the coordinate DLD structure of laser images inherent to skin histological sections of healthy rat (left columns) and that sick of cancer (right columns).

Our comparative analysis of the set of statistical, correlation and fractal parameters characterizing the distributions $N_{\min}(x)$, $\widetilde{N}(x)$, $N_{\max}(x)$ enabled us to reveal:

- tendency to growth of the amount of extreme values $\Phi_{\min}$ in the coordinate DLD distribution of laser images corresponding to the layer of skin with carcinoma (Figs 5 to 7, fragments (a) and (b));
- sequential ($N_{\max}(x) \to \widetilde{N}(x) \to N_{\min}(x)$) and more fast decrease in the correlation area of autocorrelation functions $K(\Delta x)$ characterizing the coordinate structure of extreme sampling for DLD of laser images corresponding to the histological section of healthy skin as compared with the respective parameter obtained for the samples of pathologically changed skin (Figs 5 to 7, fragments (c) and (d));
- transformation of fractal distributions $N_{\max}(x)$, $\widetilde{N}(x)$ (Figs 5 and 6, fragments (e), (f)) to the statistical one (Fig. 7, fragment (e)) obtained for the sampling $\Phi(m\times n) = 0$.

The obtained results can be related with growth of the concentration inherent to collagen proteins that form the fibrilar network (Fig. 3, fragment (b)) in the rat skin with carcinoma. This biochemical process results in

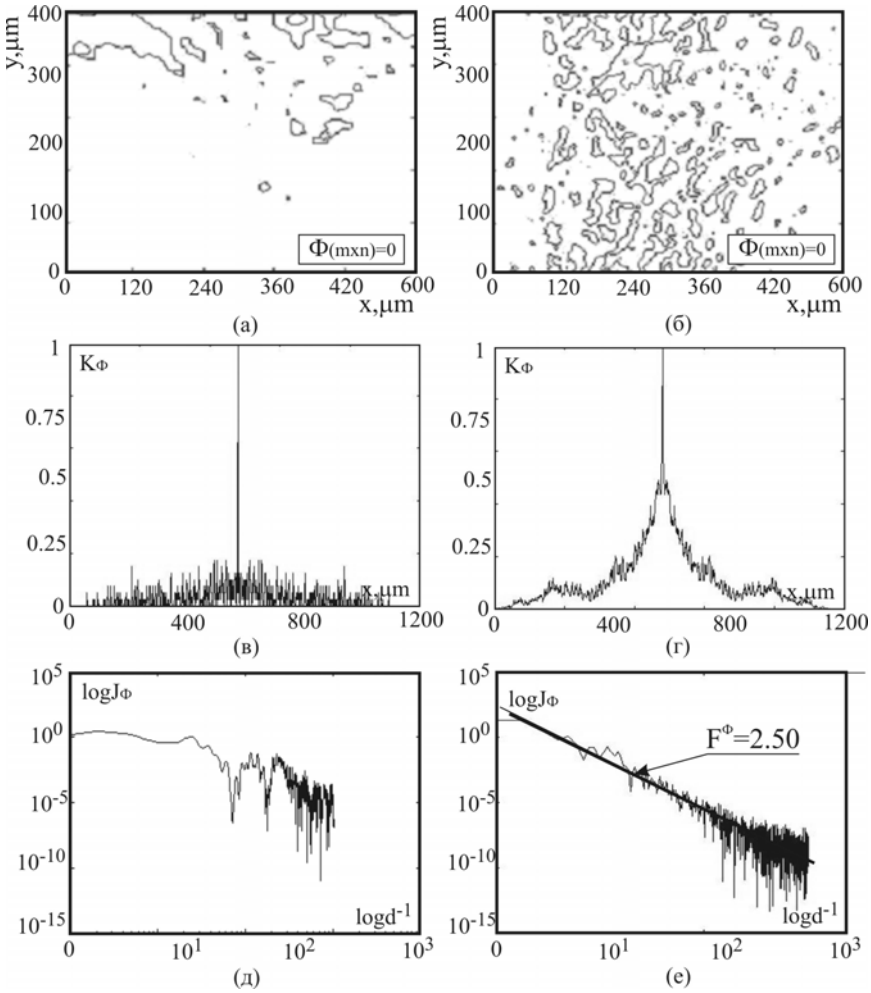

Fig. 7. Coordinate (fragments (a), (b)), correlation (fragments (c), (d)) and fractal (fragments (e), (f)) structures of the sampling $\Phi(m\times n) = 0$ for two-dimensional DLD distributions corresponding to laser images of histological sections taken from healthy rat (fragments (a), (c), (e)) and that sick with cancer (fragments (b), (d), (f)). See explanations in the text.

increasing optical anisotropy of the subsurface derma layer as well as in respective growth of the probability for extreme values $\Phi(m\times n)=0$ (relations (15) - (19)) in the coordinate DLD distribution of laser images corresponding to samples of pathologically changed skin.

In the case of healthy skin samples, the probability and, consequently, amount of these DLD values are significantly less. Using this basis, one can explain the lower values of correlation area S^{Φ} (Fig. 7, fragments (c) and (d)) as well as absence of any stable slope of the approximating curve to the logarithmic dependence $\log J(N_{\min}) - \log d^{-1}$ (Fig. 7, fragments (e) and (f)).

From the quantitative viewpoint, the dependences $N_{\min}(x)$, $\widetilde{N}(x)$, $N_{\max}(x)$ characterize statistical $Z^{\Phi}_{i=1-4}$, correlation S^{Φ} and fractal F^{Φ}, D^{Φ} parameters determined within the limits of two groups for skin samples (Table 1).

The comparative analysis of the obtained data has shown that diagnostically sensitive to the oncological state are:

- statistical moments $Z^{\Phi}_{i=1-4}(N_{\min})$ of $N_{\min}(x)$ distributions for the amount of extreme values $\Phi(m\times n)=1$, differences between them reach 2 to 3 times;
- correlation area S^{Φ} for autocorrelation functions $\widetilde{K}(\Delta x)$ and $K_{\min}(\Delta x)$, differences between them reach 2 and 5 times;
- $N_{\min}(x)$ distribution for laser images corresponding to histological sections of a healthy rat and that sick of cancer are, respectively, random and self-similar;
- dispersion D^{Φ} of the logarithmic dependences $\log J(N_{\min}) - \log d^{-1}$ in the case of pathological changes is 2-fold decreased.

Table 1. Statistical $Z^{\Phi}_{i=1-4}$, correlation S^{Φ} and fractal F^{Φ}, D^{Φ} parameters for the distributions $N_{max}(x)$, $\widetilde{N}(x)$, $N_{min}(x)$ of the amount of extreme values $\Phi(m\times n)$ in laser images of skin histological sections

$N(x)$	$N_{max}(x)$		$\widetilde{N}(x)$		$N_{min}(x)$	
	Norm (q = 21)	Cancer (q = 19)	Norm (q = 21)	Cancer (q = 19)	Norm (q = 21)	Cancer (q = 19)
Z^{Φ}_1	0.51±0.063	0.47±0.052	0.31±0.034	0.42 ± 0.045	0.09 ± 0.001	0.24 ± 0.035
Z^{Φ}_2	0.14±0.021	0.16±0.019	0.19±0.023	0.15 ± 0.018	0.43 ± 0.031	0.17 ± 0.019
Z^{Φ}_3	0.28±0.034	0.33±0.038	0.58±0.067	0.47 ± 0.065	1.65 ± 0.17	0.72 ± 0.081
Z^{Φ}_4	0.41±0.063	0.54±0.067	0.77±0.081	0.63 ± 0.072	2.11 ± 0.32	0.82 ± 0.091
S^{Φ}	0.25±0.023	0.21±0.021	0.18±0.013	0.09 ± 0.007	0.11 ± 0.013	0.02 ± 0.001
D^{Φ}	0.18±0.014	0.17±0.018	0.32±0,034	0.19 ± 0.025	0.48 ± 0.047	0.21 ± 0.035
F^{Φ}	1.98±0.016	1.93±0.07	2.17±0.05	2.03 ± 0.021	-	2.23 ± 0.031

7. Conclusions

Demonstrated in this work is the possibility to use the parameter of degree of local depolarization for describing the processes of the multiple scattering of laser radiation by optically anisotropic biological tissues. Offered is a model approach to the analysis of correlation-phase structure formation in the field of laser radiation scattered by a birefringent skin layer with rough surface. Developed and tested is the experimental method for measuring the coordinate DLD distributions in laser images of rat skin histological sections. Being based on it, the authors have determined and grounded the set of statistical, correlation and fractal criteria for diagnostics of skin cancer.

References

1. W.F. Cheong, S.A. Prahl, A.J. Welch, "A review of the optical properties of biological tissues," *IEEE J. of Quant. Elec*. **26**, 2166-2185 (1990).
2. S. A. Prahl, M. Keijzer, S. L. Jacques, and A. J. Welch. *A Monte Carlo model of light propagation in tissue. In G. J. Müller and D. H. Sliney, eds, SPIE Proceedings of Dosimetry of Laser Radiation in Medicine and Biology*, volume IS 5, pp. 102-111, (Bellingham, WA, 1989. SPIE Opt. Eng. Press).
3. J.Ellis and A.Dogariu, "Complex degree of mutual polarization," *Opt.Lett*. **29**, 536-538 (2004).
4. Jani Tervo, Tero Setala, and Ari Friberg, "Degree of coherence for electromagnetic fields," Opt. Express **11**, 1137-1143 (2003)
5. O. V. Angelsky, A. G. Ushenko, Yu. A. Ushenko, V. P. Pishak, *"Statistical and Fractal Structure of Biological Tissue Mueller Matrix Images", in Optical Correlation Techniques and Applications*, Oleg V. Angelsky, ed. (Washington: Society of Photo-Optical Instrumentation Engineers), pp. 213-266 (2007).
6. O.V. Angelsky, A.G. Ushenko, Yu.A. Ushenko, V.P. Pishak, and A.P. Peresunko, *"Statistical, Correlation, and Topological Approaches in Diagnostics of the Structure and Physiological State of Birefringent Biological Tissues", in Handbook of Photonics for Biomedical Science*, Valery V. Tuchin, ed. (USA: CRC Press), pp. 21-67 (2010).
7. Alexander G. Ushenko and Vasilii P. Pishak, *"Laser Polarimetry of Biological Tissue: Principles and Applications", in Handbook of Coherent-Domain Optical Methods: Biomedical Diagnostics, Environmental and Material Science*, Valery V. Tuchin, ed. (Boston: Kluwer Academic Publishers), pp. 93-138 (2004).
8. Alexander G. Ushenko, "Polarization structure of laser scattering fields," *Opt. Eng*. **34**, 1088-1093 (1995).
9. A.G. Ushenko, "Laser diagnostics of biofractals," *Quantum Electron*. **29**, 1078–1084, (1999).
10. O.V. Angel'skii, A.G. Ushenko, A.D. Arkhelyuk, S.B. Ermolenko, D.N. Burkovets, "Structure of matrices for the transformation of laser radiation by biofractals," *Quantum Electron.* **29**, 1074-1077 (1999).
11. O.V. Angel'skii, A.G. Ushenko A.D. Arheluk, S.B. Ermolenko, D. N. Burkovets, "Scattering of Laser Radiation by Multifractal Biological Structures," *Optics and Spectroscopy* **88**, 444-448 (2000).
12. A.G. Ushenko, "Polarization Structure of Biospeckles and the Depolarization of Laser Radiation," *Optics and Spectroscopy* **89**, 597-601 (2000).

13. A.G. Ushenko, "Stokes-correlometry of biotissues," *Laser Phys*. **10**, 1286-1292 (2000).
14. A.G. Ushenko, "The Vector Structure of Laser Biospeckle Fields and Polarization Diagnostics of Collagen Skin Structures," *Laser Phys*. **10**, 1143-1149 (2000).
15. A.G. Ushenko, "Laser polarimetry of polarization-phase statistical moments of the object field of optically anisotropic scattering layers," *Optics and Spectroscopy* **91**, 313-316 (2001).
16. A.G. Ushenko, "Polarization contrast enhancement of images of biological tissues under the conditions of multiple scattering," *Optics and Spectroscopy* **91**, 937-940 (2001).
17. A.G. Ushenko, "Laser probing of biological tissues and the polarization selection of their images," *Optics and Spectroscopy* **91**, 932-936 (2001).
18. A.G. Ushenko, "Correlation processing and wavelet analysis of polarization images of biological tissues," *Optics and Spectroscopy* **91**, 773-778 (2002).
19. A.G. Ushenko, "Polarization correlometry of angular structure in the microrelief pattern or rough surfaces," *Optics and spectroscopy* **92**, 227-229 (2002).
20. O.V. Angelsky, A.G. Ushenko, Ye.G. Ushenko, "2-D Stokes Polarimetry of Biospeckle Tissues Images in Pre-Clinic Diagnostics of Their Pre-Cancer States," *J. Holography Speckle* **2**, 26-33 (2005).
21. Oleg V. Angelsky, Alexander G. Ushenko, and Yevheniya G. Ushenko, "Complex degree of mutual polarization of biological tissue coherent images for the diagnostics of their physiological state," *J. Biomed. Opt*. **10**, 060502 (2005).
22. O. V. Angelsky, A. G. Ushenko, and Ye. G. Ushenko, "Investigation of the correlation structure of biological tissue polarization images during the diagnostics of their oncological changes," *Phys. Med. Biol*. **50**, 4811-4822 (2005).
23. Oleg V. Angelsky, Alexander G. Ushenko, Yevheniya G. Ushenko, Yuriy Y. Tomka, "Polarization singularities of biological tissues images," *J. Biomed. Opt*. **11**, 054030 (2006).
24. O.G. Ushenko, S.G. Guminetsky, A.V. Motrich, "Optical properties of urine, blood plasma and pulmonary condensate of the patients with pulmovnary form of tuberculosis," *Photoelectronics* **16**, 133-139 (2007).
25. S.H. Guminetskiy, O.G. Ushenko, I.P. Polyanskiy, A.V. Motrych, F.V. Grynchuk, "The optical method for investigation of the peritonitis progressing process," *Proc. SPIE* **7008**, 700827 (2008).
26. Alexander Ushenko, Sergej Yermolenko, Alexander Prydij, Stepan Guminetsky, Ion Gruia, Ovidiu Toma, Konstantin Vladychenko, "Statistical and fractal approaches in laser polarimetry diagnostics of the cancer prostate tissues," *Proc. SPIE* **7008**, 70082C (2008).
27. A.G. Ushenko, A.I. Fediv, Yu.F. Marchuk, "Correlation and fractal structure of Jones matrices of human bile secret," *Proc. SPIE* **7368**, 73681Q (2009).
28. A.G. Ushenko, Yu.Ya. Tomka, V.I. Istratiy, "Polarization selection of two-dimensional phase-inhomogeneous birefringence images of biotissues," *Proc. SPIE* **7388**, 73881L (2009).
29. A.G. Ushenko, A.I. Fediv, Yu.F. Marchuk, "Singular structure of polarization images of bile secret in diagnostics of human physiological state," *Proc. SPIE* **7368**, 73681S (2009).
30. S.B. Yermolenko, A.G. Ushenko, P. Ivashko, "Spectropolarimetry of cancer change of biotissues," *Proc. SPIE* **7388**, 73881D (2009).
31. A.G. Ushenko, I. Z.Misevich, V. Istratiy, I. Bachyns'ka, A. P. Peresunko, Omar Kamal Numan, and T. G. Moiysuk, "Evolution of Statistic Moments of 2D-Distributions of Biological Liquid Crystal Net Mueller Matrix Elements in the Process of Their Birefringent Structure Changes," *Advances in Optical Technologies* **2010**, 423145 (2010).